

Non-isothermal melt crystallization kinetics for ethylene–acrylic acid copolymer in diluents via thermally induced phase separation

Jun Zhang · Shuangjun Chen · Jing Jin ·
Xuming Shi · Xiaolin Wang · Zhongzi Xu

Received: 26 July 2009 / Accepted: 18 November 2009 / Published online: 4 December 2009
© Akadémiai Kiadó, Budapest, Hungary 2009

Abstract Non-isothermal crystallization kinetics of the ethylene–acrylic acid copolymer (EAA) in diluents during thermally induced phase separation (TIPS) process was investigated via differential scanning calorimetry (DSC). Diethyl phthalate (DOP), diphenyl ester (DPE), and peanut oil were used as diluents. Kinetic models, such as Jeziorny theory, Ozawa theory, and Mo's approach, were utilized for description. The effective activation energy of EAA component in mixture was calculated by Friedman's method. In the results, the Jeziorny theory and Mo's approach could obtain good linear fitting relationship with the primary crystallization behavior of EAA, but the Ozawa theory failed to get a suitable result. The homogeneous nucleation of EAA proceeded at the end of liquid–liquid phase separation, while the non-isothermal crystallization developed within a solid–liquid phase separation environment. In the mixtures, the molecular weight, polar groups, and conformation of the diluent molecules would affect the nucleation of EAA, and its growth rate. Comparing with the non-isothermal crystallization of neat EAA, EAA in diluents obtained a higher Avrami index n , and comparatively lower crystallization rate. Peanut oil facilitated the homogeneous nucleation of EAA, leading to a higher melting peak temperature of EAA in the subsequent melting endotherms. The largest EAA's Avrami index

obtained in peanut oil also indicated a higher crystal growth dimensional geometry. The crystallization rate and crystallinity of EAA during the non-isothermal process decreased in the sequence: EAA/DPE > EAA/DOP > EAA/peanut oil.

Keywords Non-isothermal crystallization · Ethylene–acrylic acid copolymer · Diluents · Crystallization kinetic parameters

Introduction

Up to now, a lot of engineering and commodity plastics, such as polypropylene (PP) [1, 2], polyethylene (PE) [3–5], poly(vinylidene fluoride) (PVDF) [6–8] and polystyrene (PS) [9], etc., have been applied for micro-porous membranes preparation via thermally induced phase separation (TIPS) method. The membranes made from these materials are generally hydrophobic, which may limit the application area of these membranes due to solute adsorption and pore blocking. In order to make stable hydrophilic micro-porous membrane, co-polymer with hydrophilic components, such as poly(ethylene-co-vinyl alcohol) (EVOH) [10], ethylene–acrylic acid copolymer (EAA) [11, 12], have been used as the membrane materials. Furthermore, the interaction between crystallization kinetics of the polymer component and the ambient TIPS process plays a crucial role in the formation of micro-porous membranes. Interactions between polymer and the diluent varied dynamically, which influence the crystallization properties of polymer content crucially and further the structure and property of micro-porous membrane. As one of the typical semi-crystalline polymers, the crystallization behavior of EAA component during the TIPS process is of great importance. However, few emphases are

J. Zhang (✉) · S. Chen · J. Jin · X. Shi · Z. Xu
College of Materials Science and Engineering, Nanjing
University of Technology, Nanjing 210009, China
e-mail: zhangjun@njut.edu.cn

X. Wang
Department of Chemical Engineering, Tsinghua University,
Beijing 100084, China

focused on the non-isothermal crystallization behavior and kinetics in the polymer/diluent mixtures.

The crystallization kinetic studies of PE [13–15] and ethylene copolymer [16] have been widely emphasized, especially under non-isothermal condition. Influences from continuously changing ambient temperature, heat transmission lags, and thermal gradients within samples must be taken into account, which are all vital factors referring to the overall crystallization properties of polymer. In our previous study, the non-isothermal crystallization behavior of EAA with different acrylic acid (AA) content has been discussed [17]. The crystallization rate of the primary stage was significantly influenced by the competitive mobility of chains. While the crystallization rate in the secondary stage was determined by the AA content in copolymers. Factors mentioned above could be affected by the ambient condition variation in different EAA/diluents systems. In this study, EAA possessing 8 wt% of AA content was utilized to be mixed with three different diluents: dioctyl phthalate (DOP), diphenyl ester (DPE), and peanut oil. Differential scanning calorimetry (DSC) was employed to study the non-isothermal crystallization of EAA/diluent mixtures under different cooling rates. The crystallization kinetics was adequately described via the Jeziorny theory, the Ozawa theory, and a new combination of the Avrami and Ozawa methods developed by Mo. The effective activation energy of EAA component in mixture was calculated by Friedman's method. The non-isothermal crystallization and subsequent melting behaviors were also analyzed to reveal

the relations between phase separation and the crystallization kinetics.

Experimental

Materials

EAA 3002 was obtained from the Dow Chemical Company, USA. Composition in weight fraction of EAA copolymer was ethylene/acrylic acid = 92/8. The density is 0.936 g cm^{-3} . The AA co-monomer can be considered to be randomly distributed along the copolymer chains.

Dioctyl phthalate (DOP) was purchased from Lingfeng Chemical Reagent Co., Ltd. (China). DPE was purchased from Sinopharm Chemical Reagent Co., Ltd. (China). Peanut oil without antioxidant was supplied by Shandong Luhua-Group Co., Ltd. (China). Peanut oil is a homogeneous mixture of linoleic acid, oleic acid, and some of their glyceride. All of these chemicals (DPE, DOP, and peanut oil) were used without any further purification. Their molecular structures were listed in Table 1.

Preparation of EAA/diluent mixtures

The polymer and diluents with a mass ratio of EAA/diluent = 20/80 were weighed into a glass test tube, and homogeneous polymer/diluent mixtures were obtained after the tube was heated in an oil bath at 453 K for 4 h under sufficient stirring. Then, they were cooled at the room temperature. Finally, the solidified polymer/diluent mixtures (EAA/DPE, EAA/DOP, and EAA/peanut oil) were obtained.

DSC measurements

The non-isothermal crystallization and the subsequent melting of three EAA/diluent samples with different diluents were carried out via a DSC apparatus (model Pyris 1, PerkinElmer, USA). Samples weighing 8–10 mg were applied for the DSC characterization. Argon gas purge with a flux of 25 mL min^{-1} was used to prevent thermal degradation of samples during the scanning. In order to remove the volatile impurities and erase the former thermal history, the EAA/diluent mixtures were first heated up to 423 K at a rapid heating rate of 40 K min^{-1} and kept at 423 K for 5 min. Then, they were cooled down from 423 to 273 K at the rate of 2.5, 5, 10, and 20 K min^{-1} to obtain the non-isothermal crystallization curves, respectively. The second heat running was made from 273 to 423 K at 10 K min^{-1} .

In our previous study [18, 19], the crystallinity (X_c) of EAA was calculated as follows:

Table 1 Molecular structures of three diluents

Diluent	Molecular structure
DPE	
DOP	
Peanut oil	Oleic acid Linoleic acid and their glyceride mixtures

$$X_c = \frac{\Delta H_f / \Phi}{\Delta H_f^*} \times 100\%, \quad (1)$$

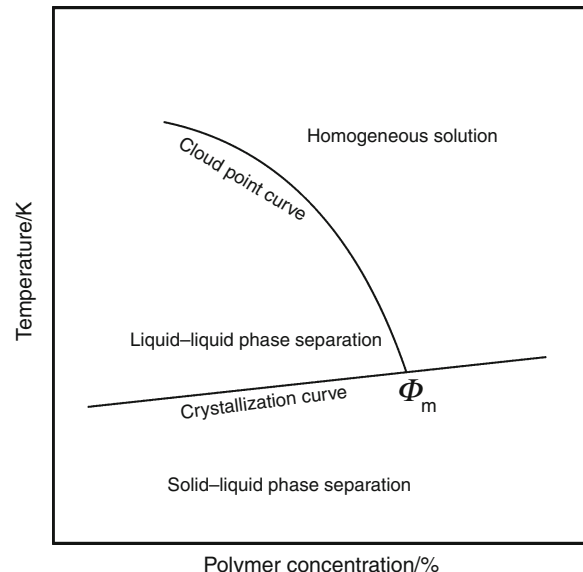
where ΔH_f^* is the enthalpy of fusion of the perfect PE crystal, ΔH_f is the enthalpy of fusion of the EAA/diluent mixtures measured in DSC, and Φ is the weight fraction of EAA in the EAA/diluent mixtures. The value of ΔH_f^* for PE is 277.1 J g^{-1} in literature [20].

Results and discussion

Phase diagram background

Scheme 1 illustrates the typical phase diagram of a semi-crystalline polymer/diluent mixture at various given self-conditions and external ambient temperatures. According to the phase diagram, there are three regions when temperature and initial polymer concentration of the polymer/diluent mixture are different. They are homogenous solution region, liquid–liquid phase separation region and solid–liquid phase separation region, respectively. The monotectic point [21, 22] (Φ_m) is the intersection of a liquid–liquid phase separation curve and a crystallization curve. As an approximation, the cloud point curve is assumed to be a two phase coexistence curve [23]. Above the cloud point curve, it is the one-phase region where a homogeneous solution of polymer/diluent exists. Bounded by the cloud point curve and the crystallization curve to the left region of Φ_m is the liquid–liquid phase separation region. Cooling a homogenous polymer/diluent mixture ($C = 20\% < C_{\Phi_m}$), the mixture system will present liquid–liquid phase separation when the temperature is below the cloud point value. Then, the homogenous solution separates into two liquid phases in thermodynamic equilibrium. Below the crystallization curve, the polymer solidifies. The solid–liquid phase separation region occurs to the right of Φ_m . In the process of solid–liquid phase separation, it occurs via crystallization of the polymer out of the homogeneous solution.

In our previous study, phase diagrams of EAA/diluents (DPE, DOP, and peanut oil etc.) were obtained [24]. They were typical diagrams of semi-crystalline polymer/diluent system with weak inter-molecular interactions. In the order of EAA/DPE, EAA/DOP, and EAA/peanut oil, the cloud point curve shifted to a lower temperature, whereas the crystallization temperature was not influenced much by the diluents type except DPE. The phase separation during the TIPS is determined by the polymer concentration in the system. The C_{Φ_m} of EAA/DPE mixture was ranged from 45 to 50 wt%, while for the mixtures of EAA/DOP and EAA/peanut oil, the C_{Φ_m} decreased to a value ~ 35 wt%. Because



Scheme 1 Typical phase diagram of semi-crystalline polymer/diluent mixture

the TIPS method is a non-isothermal process, it is essential to investigate the crystallization behavior of polymer component in the phase separation process. Therefore, in this study, the non-isothermal processes under different cooling rates at 2.5, 5, 10, and 20 K min^{-1} were investigated. The total polymer concentration was 20 wt%, which was lower than monotectic point C_{Φ_m} . Thus, the liquid–liquid phase separation and solid–liquid phase separation could occur during the non-isothermal crystallization, and the influence of diluent type on the non-isothermal crystallization kinetics can be investigated.

Non-isothermal crystallization analysis

Exotherms of three mixtures' non-isothermal crystallization at various cooling rates are illustrated in Fig. 1. Increasing of cooling rate leads to the lag in crystallization behavior. Exothermic peak temperature T_p shifts to a lower position with an increase of the cooling rate. In addition, the crystallization peak becomes narrower as the cooling rate increases. Data obtained in Fig. 1 are listed in Table 2. It shows that the faster cooling rate leads to a higher value of crystallization enthalpy. The T_c^p of EAA in EAA/diluents system are all lower than the value in neat EAA [17] (T_c^p arranged between 353.7 and 360.4 K), indicating polymer molecules in diluents are isolated from each other, and their crystallization behavior are delayed to some extent. The onset crystallization temperature of EAA in EAA/peanut oil system is higher than that in DOP and DPE diluents. This indicates a facilitation of

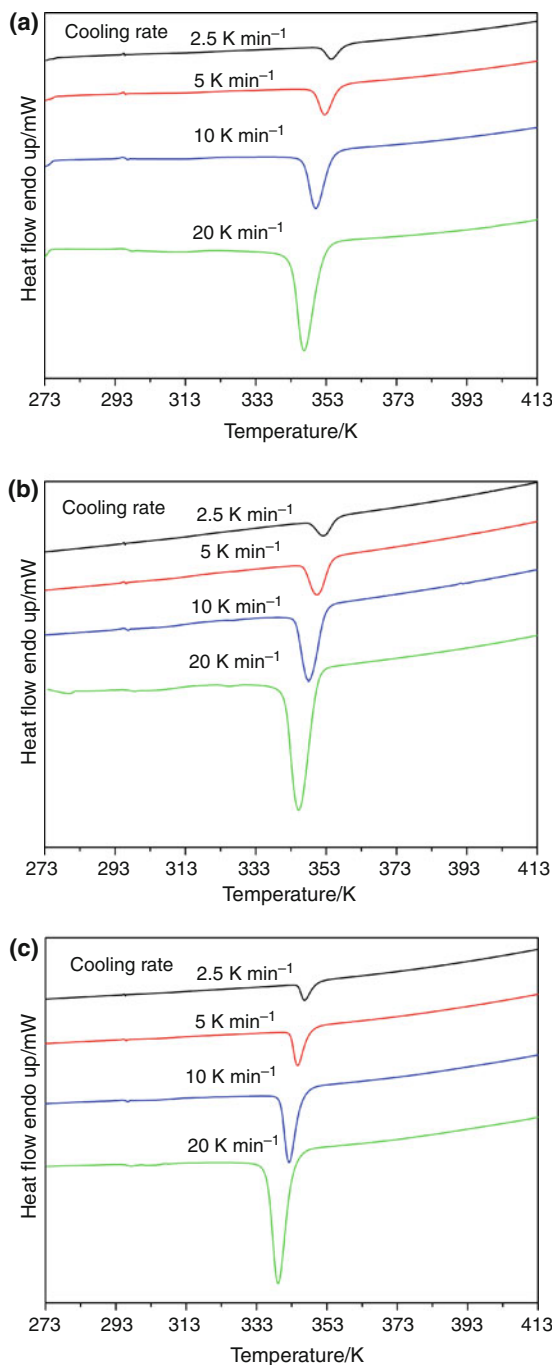


Fig. 1 Non-isothermal crystallization DSC curves for three EAA/diluent mixtures at various cooling rates. **a** Peanut oil, **b** DOP, and **c** DPE

nucleation in peanut oil, due to the better polymer chains insulation effect.

Jeziorny theory

The heating flow of crystallization process was recorded as a function of temperature. The relative crystallinity X_t is formulated as [25]

Table 2 Non-isothermal crystallization DSC results for three EAA/diluent mixtures

Sample	$D/\text{K min}^{-1}$	T_c^{on}/K	T_c^p/K	T_c^f/K	$\Delta T_c/\text{K}$	$\Delta H_c/\text{J g}^{-1}$
EAA/peanut oil	2.5	358.4	354.6	351.7	6.7	12.20
	5	356.7	352.6	349.6	7.1	12.51
	10	354.8	350.0	346.7	8.1	13.57
	20	352.2	346.8	343.2	9.0	14.10
EAA/DOP	2.5	356.0	352.2	348.5	7.5	13.62
	5	354.5	350.3	346.3	8.2	14.25
	10	352.7	348.1	344.3	8.4	14.31
	20	350.8	345.2	341.3	9.5	14.80
EAA/DPE	2.5	349.8	346.7	344.8	5.0	13.10
	5	348.0	344.7	342.7	5.3	15.47
	10	345.9	342.2	339.6	6.3	17.20
	20	343.3	339.0	336.0	7.3	18.18

D cool rate, T_c^{on} onset crystallization temperature of EAA, T_c^p peak crystallization temperature of EAA, T_c^f final crystallization temperature of EAA; $\Delta T_c = T_c^{\text{on}} - T_c^f$, ΔH_c crystallization enthalpy of EAA

$$X_t = \frac{\int_{T_0}^T (dH_c/dT)dT}{\int_{T_0}^{T_\infty} (dH_c/dT)dT} \times 100\%, \quad (2)$$

where the T_0 and T_∞ represent the temperature at the onset and the end of the crystallization process, respectively. However, dH_c stands for the enthalpy of the crystallization released during an infinitesimal temperature range dT .

Figure 2 illustrates the development of X_t to the T of all samples. The horizontal T -axis in Fig. 2 can be transformed into the crystallization time t -axis as shown in Fig. 3. Crystallization time can be calculated in the following equation, in which D stands for the cooling rate (2.5, 5, 10, and 20 K min^{-1}).

$$t = |T_0 - T|/D \quad (3)$$

The growth of relative crystallinity X_t versus the passing time t gives rise to the definition of crystallization half time $t_{1/2}$, which corresponds to 50% of the crystal conversion process. This could be used as a criterion of the crystallization rate. The shorter $t_{1/2}$, the faster macromolecules crystallization rate.

Avrami equation [26–28], which has been commonly utilized in describing isothermal crystallization kinetics, is given as

$$1 - X_t = \exp(-Z_t t^n), \quad (4)$$

where Z_t represents the crystallization rate constant, involving composition of both nucleation and growth rate parameters. Parameter n stands for Avrami exponent, which refers to the mechanism of crystalline growth. The equation could be transformed into the double logarithm style as follows:

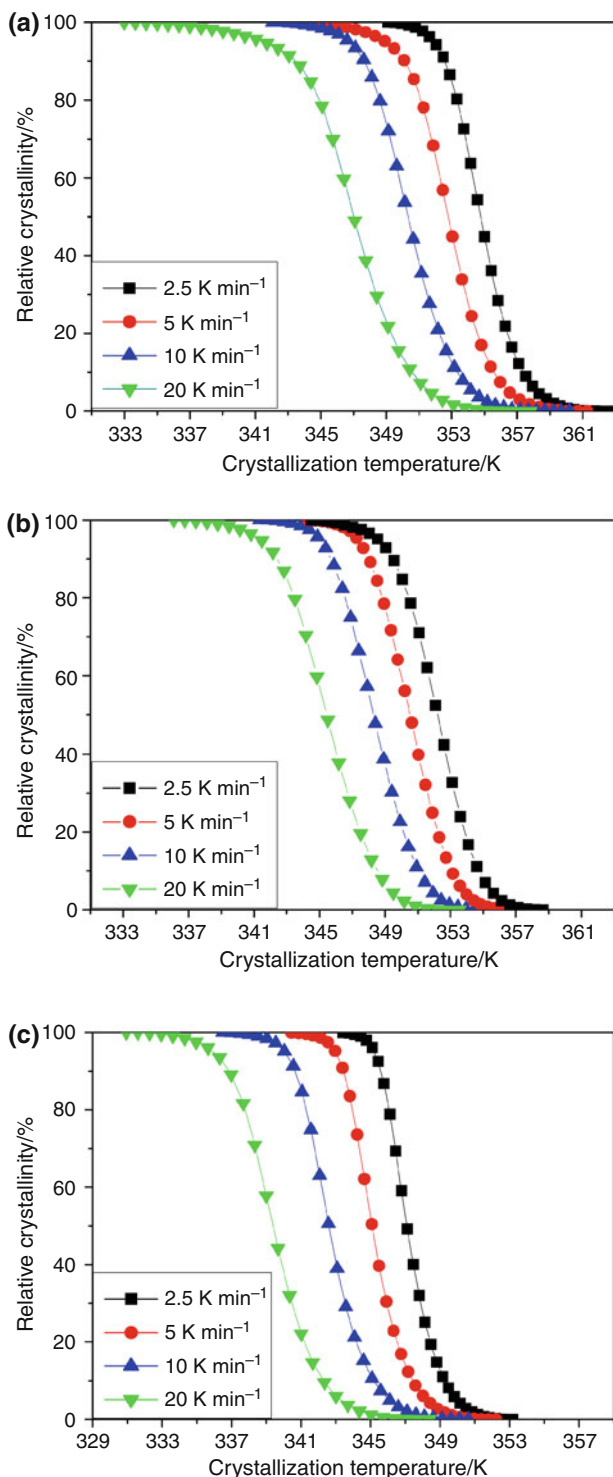


Fig. 2 Plots of relative crystallinity versus crystallization temperature for three EAA/diluent mixtures during non-isothermal crystallization processes. **a** Peanut oil, **b** DOP, and **c** DPE

$$\log[-\ln(1 - X_t)] = \log Z_t + n \log t. \quad (5)$$

Drawing the straight line given by Eq. 4 enables one to obtain the Avrami exponent n and the crystallization rate

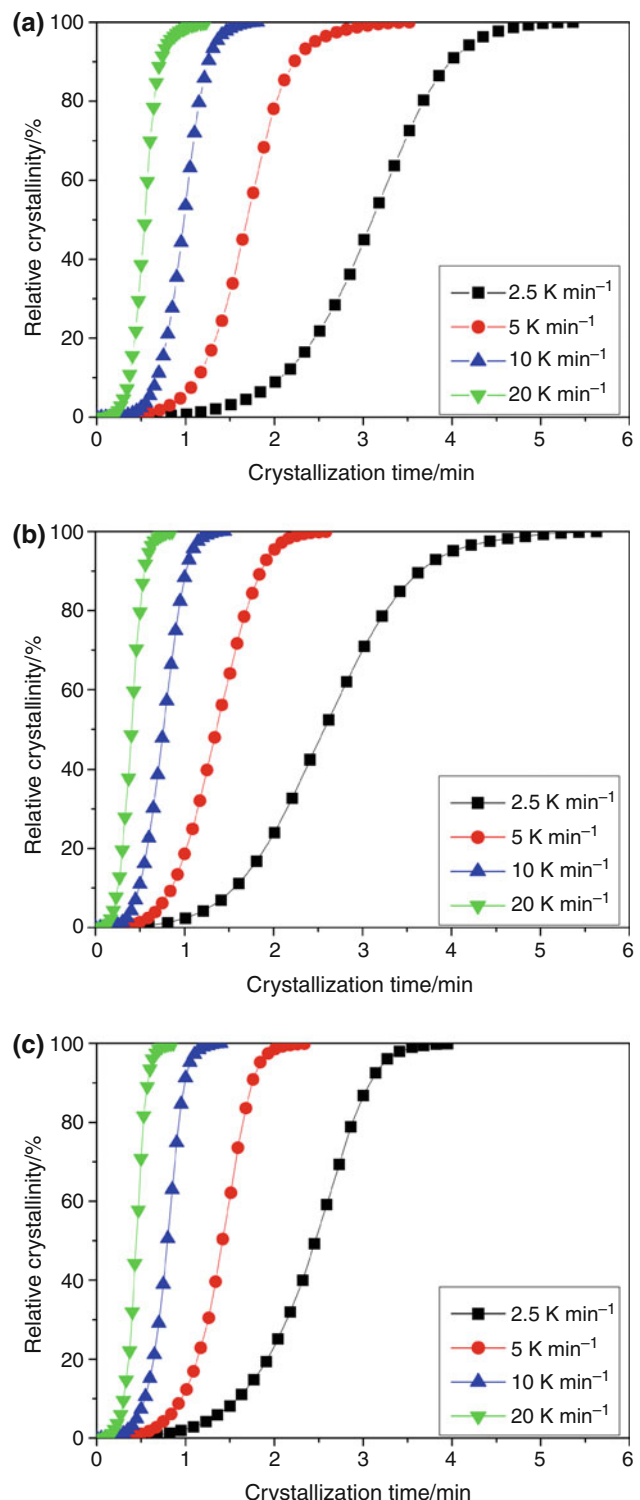


Fig. 3 Plots of relative crystallinity versus crystallization time for three EAA/diluent mixtures during the non-isothermal crystallization processes. **a** Peanut oil, **b** DOP, and **c** DPE

constant Z_t from the slope and the intercept, respectively. Considering the non-isothermal crystallization character investigated in this study, the value of Z_t should not be

appropriate to describe the dynamic non-isothermal situation. Considering the influence of cooling rate D on gradually decreasing temperature condition, the rate parameter should be modified as follows:

$$\ln Z_c = \ln Z_t / D \quad (6)$$

Z_c , which characterizes non-isothermal process, is modified by Jeziorny [29]. Utilizing modified Avrami equation, it would be easy to characterize non-isothermal crystallization kinetics details of these binary mixtures. Based on the experiment information from Fig. 3, plots of $\log(-\ln(1 - X_t))$ versus $\log(t)$ of the linear data segments for EAA/diluent samples are given in Figs. 4 and 5. Two stages of crystallization in these curves are perceptible. The first part shows approximate linear relationship. Whereas the later stage of all traces deviates from the former linear direction. Phenomenon above was observed prevalently in literatures [30–32]. The secondary crystallization stage processed after the spherulites impingement, which was apparently slower than the primary stage. In the diluted mixture, the crystals of EAA grow freely in a space of amorphous phase prior to impingement of crystals, until they reach the maximum of crystallization rate corresponding to T_c^P . The further secondary stage may take place in inter-molecular regions and proceed at a much slower rate after the impingement of adjacent spherulites.

Discrete data points were fitted to linear style and approximate straight lines are obtained (with iteration fitting *Adjust r*² > 0.987). Even the initial stage of plots, slight data deviation can be observed in Fig. 4. This implies the crystallization rate constant Z_c depends upon crystallization temperature to some extent. The final evaluation results are listed in Table 3. The acrylic acid units introduced into copolymer texture would hinder chain folding during crystallization. When mixed with diluents, crystallization behavior of EAA takes place together with the solid–liquid phase separation process. Liquid phase diluent molecules placed in this binary mixture results in an insulation of polymer chains with each other. Spherulites could grow in a larger degree of freedom. Avrami exponent n arranges between 3.5 and 4.5 in all EAA/diluents systems, higher than that in the neat polymer [17] (n grew from 3.3 to 3.8), which indicates the crystal could be approximation of homogenous nucleation with three-dimensional (spherulitic) growth. The values of $n > 4$ at various cooling rates may be due to the spherulites' impingement and crowding, or a more complicated nucleation type and growth form of spherulite [33]. As reported in the literature, cooling condition affects the crystal growth geometry mode [34]. In this experiment, the increase in cooling rate leads to a higher n value, indicating the crystal grows in more dimensions.

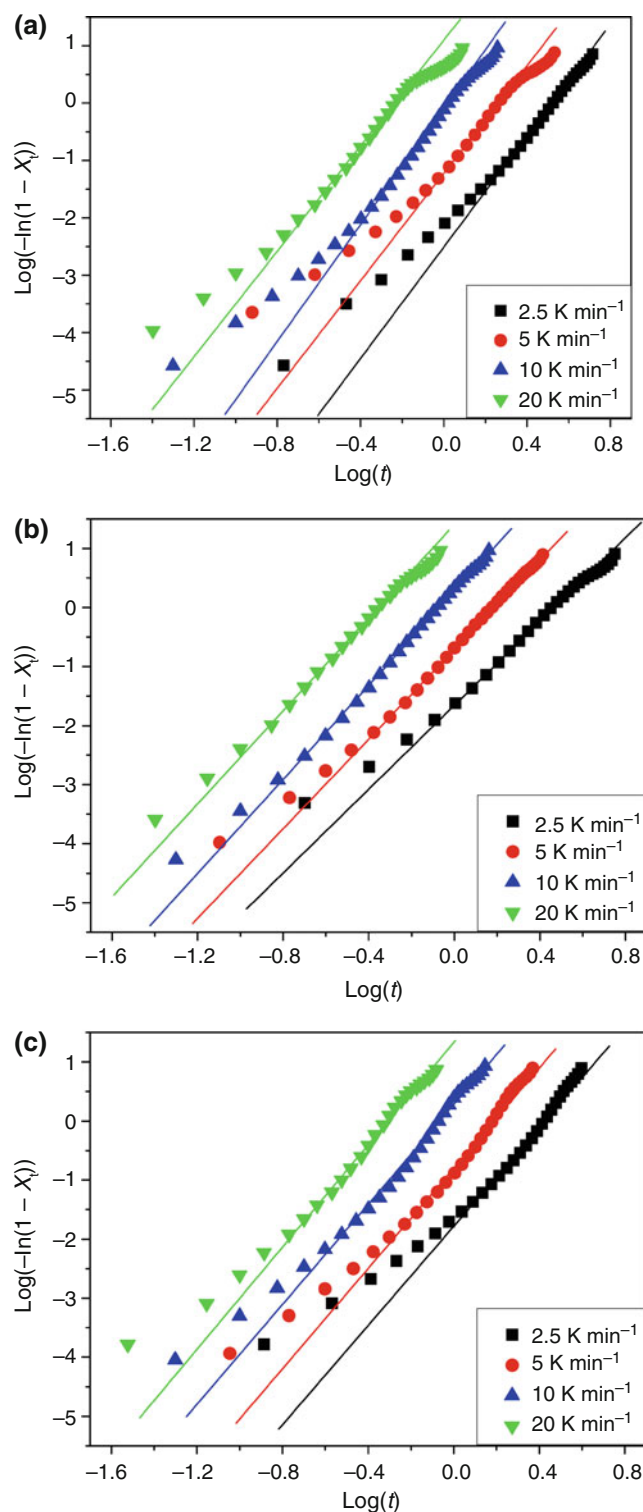


Fig. 4 Plots of $\log(-\ln(1 - X_t))$ versus $\log(t)$ for three EAA/diluent mixtures during the non-isothermal crystallization process. **a** Peanut oil, **b** DOP, and **c** DPE

The non-isothermal crystallization rate constant Z_c grows along with the increasing cooling rate. Considering the influence from different diluents, Z_c of EAA in mixtures all

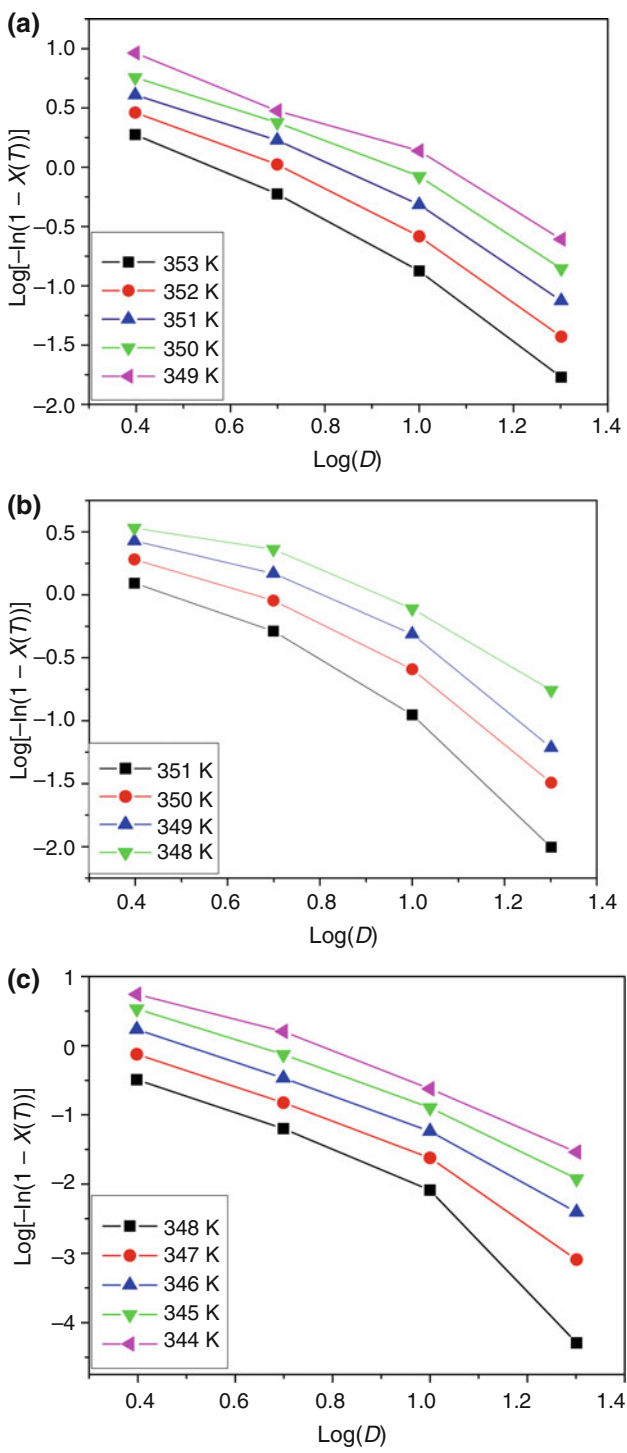


Fig. 5 Plots of $\log(-\ln(1 - X(T)))$ versus $\log(D)$ for three EAA/diluent mixtures during the non-isothermal crystallization process. **a** Peanut oil, **b** DOP, and **c** DPE

keeps slightly lower than the case of neat copolymer. Similar variation in $t_{1/2}$ is also observed; the values of polymer in mixtures stay steadily higher than that in the single component case [17]. Inter-molecular interaction

Table 3 Non-isothermal crystallization kinetic parameters from Jeziorny theory

Sample	$D/K \text{ min}^{-1}$	Z_c/min^{-1}	n	$\text{Adj. } r^2$	$t_{1/2}/\text{min}$
EAA/peanut oil	2.5	0.139	3.87	0.99315	3.12
	5	0.592	4.18	0.99199	1.69
	10	0.953	4.43	0.99232	0.99
	20	1.107	4.08	0.99057	0.54
	2.5	0.221	3.58	0.99883	2.57
EAA/DOP	5	0.731	3.83	0.99814	1.35
	10	1.078	4.16	0.99926	0.77
	20	1.176	3.96	0.99944	0.40
	2.5	0.229	3.49	0.99240	2.47
EAA/DPE	5	0.678	3.74	0.98698	1.42
	10	1.049	4.08	0.99172	0.80
	20	1.168	4.36	0.98711	0.45

between the liquid diluents and EAA results in some kind of tangling effect, diluent molecule with complex structure would slow down the folding back, and arranging of EAA chain segments. Comparing with other two diluents, components of peanut oil have the largest molecular weight, the longest chain-like structure, and the polar carboxyl on the diluent molecules. It could also impose stronger interaction with acrylic acid groups on EAA's chain segments. In accordance with the system's largest half crystallization time $t_{1/2}$, Z_c of EAA in EAA/peanut oil system is smallest (Table 3). Therefore, peanut oil hinders EAA chain's arranging ability apparently, leading to the slowest crystallization rate in EAA/peanut oil binary mixture.

Ozawa theory

Ozawa equation is also frequently used in non-isothermal crystallization kinetic researches. By assuming that the non-isothermal crystallization process may be composed of infinitesimally small isothermal crystallization steps, Ozawa [35] applied the Avrami equation into the process of non-isothermal crystallization, as follows:

$$1 - X(T) = \exp \left[-\frac{K(T)}{|D|^m} \right] \quad (7)$$

$$\log[-\ln(1 - X(T))] = \log K(T) - m \log D, \quad (8)$$

where D is the cooling rate as former, $K(T)$ is the function related to the crystallization rate that indicates how fast crystallization proceeds, and m is the Ozawa index which depends on the dimension of crystal growth, which is another variation of Avrami index. According to Ozawa's theory, the relative crystallinity $X(T)$ at given temperature can be calculated from equation above. If Ozawa equation is able to

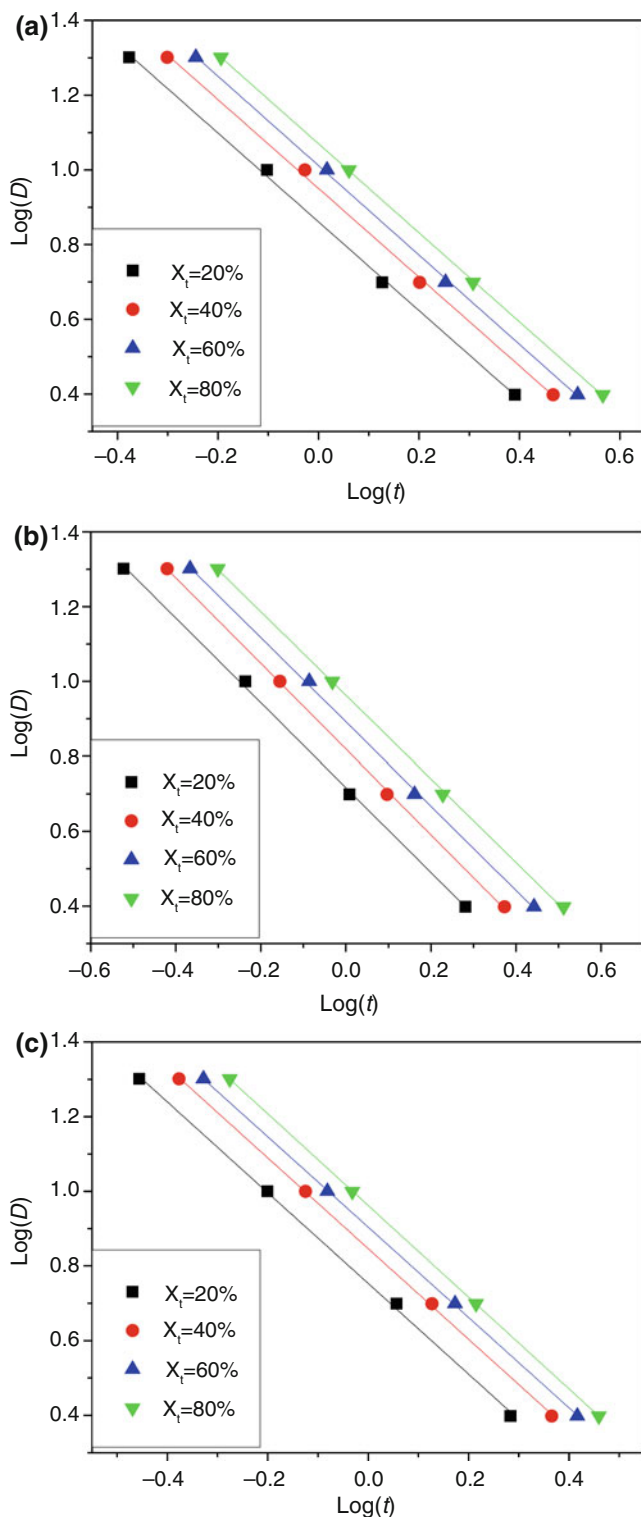


Fig. 6 Plots of $\log(D)$ versus $\log(t)$ for three EAA/diluent mixtures during the non-isothermal crystallization process. **a** Peanut oil, **b** DOP, and **c** DPE

describe this polymer/diluent mixture system, a linear relationship should be yield when $\log[-\ln(1 - X(T))]$ is plotted against $\log(D)$.

Table 4 Non-isothermal crystallization kinetic parameters from Mo's method

Sample	$X_t/\%$	$F(T)$	a	$Adj. r^2$
EAA/peanut oil	20	7.263	1.187	0.99840
	40	8.924	1.188	0.99830
	60	10.267	1.196	0.99934
	80	11.750	1.192	0.9999
EAA/DOP	20	5.206	1.132	0.99880
	40	6.597	1.144	0.99957
	60	7.798	1.125	0.99908
	80	9.184	1.115	0.99954
EAA/DPE	20	5.667	1.215	0.99871
	40	7.026	1.214	0.99973
	60	8.021	1.210	0.99991
	80	9.165	1.228	1.00000

However, analysis in this theory is based on the experimental data which represents widely varying physical exothermal process of binary mixture. The difference between various states of progress was neglected in Ozawa's model. As shown in Table 2, the various cooling rates affect the crystallization behavior apparently in the mixtures. Heat flow data of EAA/peanut oil at 354.6 K in exotherm of $D = 2.5 \text{ K min}^{-1}$ corresponds to the peak position of thermal trace, whereas in the curve of $D = 20 \text{ K min}^{-1}$, the corresponding crystallization process has not begun at this time. The given temperature points of four thermal traces refer to different non-isothermal crystallization progress. Ozawa [35] and some other researchers [36] have clarified that this model lacked enough consideration of the influence from secondary crystallization in the overall crystallization process. This could explain the failure of Ozawa's model.

Mo's method

As the Ozawa analysis is not suitable to describe the non-isothermal crystallization kinetics of EAA/diluent mixture system. Attempts were made by Mo [37, 38] via combining the Avrami equation (Eq. 5) with the Ozawa model (Eq. 8).

$$\log Z_t + n \log t = \log K(T) - m \log D \quad (9)$$

$$\log D = \frac{1}{m} \log \left[\frac{K(T)}{Z_t} \right] - \left(\frac{n}{m} \right) \log t, \quad (10)$$

where assuming the $F(T) = [K(T) \cdot Z_t^{-1}]^{1/m}$ and $a = n/m$. Parameter $F(T)$ is denoted as the value of cooling rate, which has to be chosen at a unit crystallization time when the measured sample amounts to a certain degree of crystallinity. Parameter a represents the ratio of Avrami

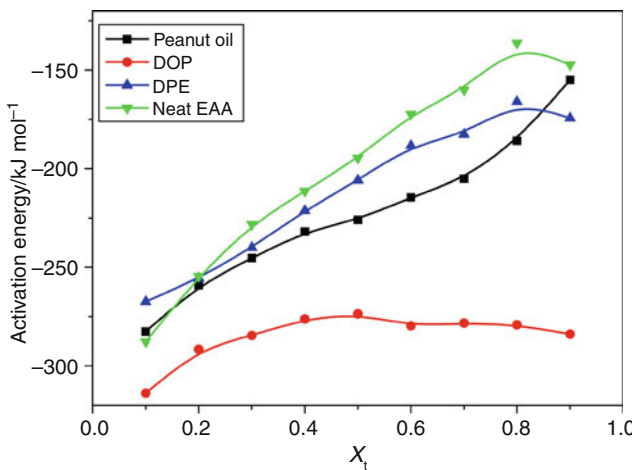


Fig. 7 Activation energy of EAA in different mixtures

exponent n to the Ozawa exponent m . Thus, the final form of Mo's approach is obtained as

$$\log D = \log[F(T)] - a \log t. \quad (11)$$

Data corresponding to relative crystallinity X_t at 20, 40, 60, and 80% are chosen for calculation; the iterative interpolation gives good linear fits results. Figure 6 presents plots of $\log(D)$ against $\log(t)$ as indicated. Evaluated results of $F(T)$ and a are listed in Table 4. It is clear that $F(T)$ grows systematically along with the increased relative crystallinity. This implies that at a given unit crystallization time, a higher cooling rate is needed to obtain higher crystallinity. The EAA/peanut oil system has the highest $F(T)$ value at a fixed value of X_t (Table 4). The highest $F(T)$ value in each point implies EAA/peanut oil system has the slowest crystallization rate. And, the dimension index ratio (a) fluctuates slightly between 1.1 and 1.2. In our previous study of neat EAA3002, $F(T)$ of $X_t = 20\%$ was 4.15, lower than the corresponding value in each diluted systems. This suggests that to obtain the specific relative crystallinity in a unit time, EAA in diluent needs a larger cooling condition.

Crystallization activation energy

In our previous study of the non-isothermal crystallization kinetics of EAA with various AA content [17], the crystallization activation energy (ΔE) was estimated via Kissinger's model [39]. However, recent studies by Vyazovkin [15, 40–42] proposed that dropping the negative sign of cooling process in such mathematic approach resulted in physical definition errors of ΔE . In this study, the differential iso-conversional method of Friedman is appreciated to estimate the energy thresholds. For a more objective

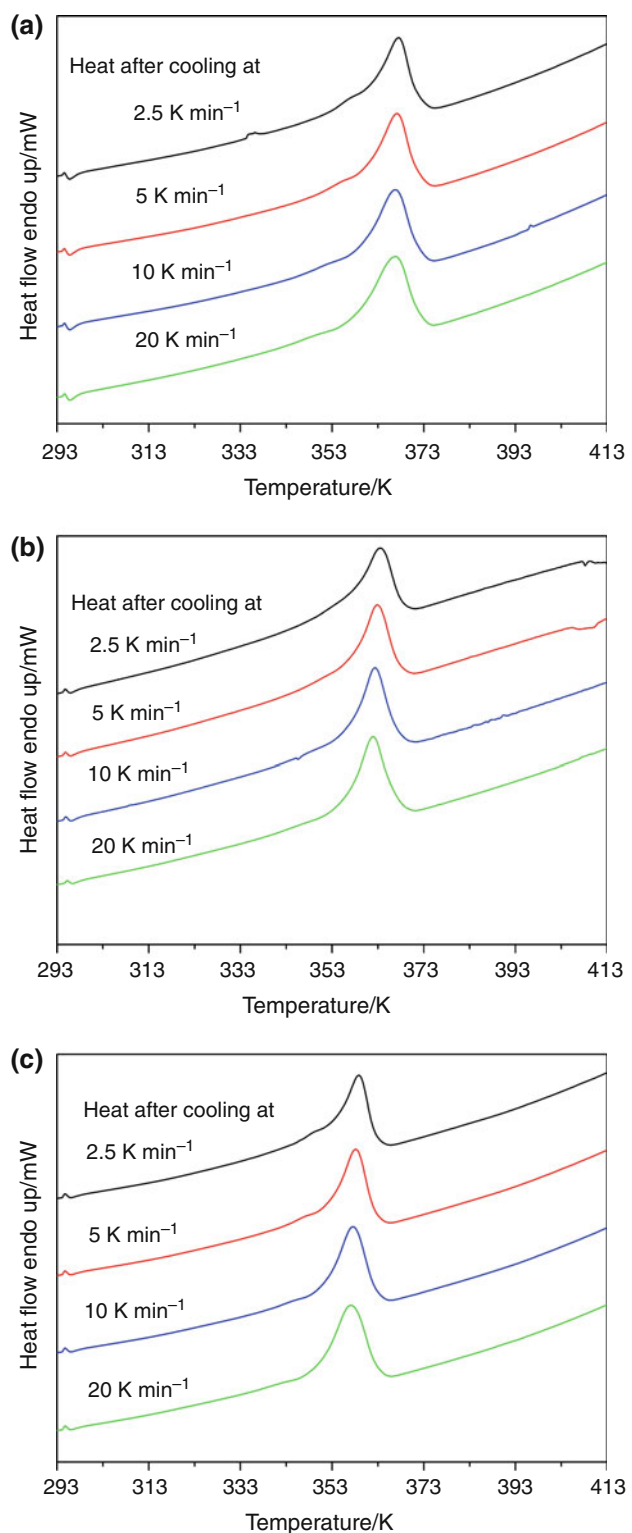


Fig. 8 Subsequent melting curves of three EAA/diluent mixtures after non-isothermally crystallized at various cooling rates. **a** Peanut oil, **b** DOP, and **c** DPE

comparison, the ΔE of neat EAA3002 was also re-calculated based on data from our previous studies [17]. The Friedman equation is given as

Table 5 Subsequent melting DSC results of three EAA/diluent mixtures after non-isothermal crystallization

Sample	$D/\text{K min}^{-1}$	$T_{\text{m}}^{\text{on}}/\text{K}$	$T_{\text{m}}^{\text{p}}/\text{K}$	$T_{\text{m}}^{\text{f}}/\text{K}$	$\Delta T_{\text{m}}/\text{K}$	$X_{\text{c}}/\%$
EAA/peanut oil	2.5	359.0	367.4	372.1	13.1	22.8
	5	358.5	367.1	371.9	13.3	23.0
	10	357.7	366.6	372.0	14.3	23.4
	20	356.7	366.8	372.3	15.6	23.7
EAA/DOP	2.5	355.3	363.3	368.1	12.8	25.4
	5	356.0	362.9	367.9	12.0	25.7
	10	355.8	362.2	368.2	12.4	26.1
	20	355.0	361.9	368.1	13.0	26.0
EAA/DPE	2.5	351.8	358.9	362.8	11.0	27.3
	5	351.3	358.0	363.3	12.0	27.7
	10	350.5	357.5	362.9	12.5	28.5
	20	349.4	357.0	363.1	13.7	28.7

D cooling rate, T_{m}^{on} onset melting temperature of EAA, T_{m}^{p} peak melting temperature of EAA, T_{m}^{f} : final melting temperature of EAA, $\Delta T_{\text{m}} = T_{\text{m}}^{\text{p}} - T_{\text{m}}^{\text{on}}$, X_{c} crystallinity of EAA

$$\ln\left(\frac{dX_t}{dt}\right)_{X_t} = A - \frac{\Delta E}{R \cdot T} \quad (12)$$

where the R is the universal gas constant ($8.314 \text{ J mol}^{-1} \text{ K}^{-1}$). A is an arbitrary pre-exponential parameter, and dX_t/dt and T represent the crystallization rate and the corresponding temperature at a given relative crystallinity (X_t), respectively. The effective activation energy barrier at a given X_t can be derived from the slope of the plot of $\ln(dX_t/dt)$ against $1/T$. Finally, the dependence of ΔE on the variation in X_t was drawn in Fig. 7.

ΔE increased gradually with the growth in X_t in all samples. Within the extent of $X_t = 10\text{--}90\%$, ΔE varied from -287.70 to $-147.27 \text{ kJ mol}^{-1}$ in neat EAA, from -282.61 to $-154.86 \text{ kJ mol}^{-1}$ in EAA/peanut oil system, from -313.85 to $-283.90 \text{ kJ mol}^{-1}$ in EAA/DOP system and from -267.43 to $-174.33 \text{ kJ mol}^{-1}$ in EAA/DPE system, respectively. It was easier for polymer to initialize crystallization at the beginning of cooling, while it became more difficult as the progress proceeded. Comparing with EAA in diluents mixtures, such growth tendencies in ΔE was more remarkable. This might be explained by the isolation effect from diluents, which insulated polymer chain sequences from tangle. EAA/DOP system possessed the lowest ΔE values through the entire crystallization process, indicating that the DOP molecules restrained the energy threshold increasing effectively.

Melting behavior

Endotherms of all EAA/diluent systems are plotted in Fig. 8. Each melting endothermal peak corresponds to a

specific lamellae thickness in crystalline texture [43–45]. The higher melting temperature refers to the thicker lamellae of EAA.

Table 5 summarizes the detailed melting results in Fig. 8. It reveals that the melting peak temperature T_{m}^{p} of EAA/diluent system decreases in the order of EAA/peanut oil, EAA/DOP, and the EAA/DPE. Increasing of cooling rate gives rise to a wider melting endothermal temperature region, which indicates a wider distribution of lamellae thickness. Crystallinity of EAA in EAA/DPE system has the highest level, around 27.3–28.7%. EAA/DOP system has a lower value around 25.4–26.0%. The lowest crystallinity is obtained in the EAA/peanut oil mixture range between 22.8 and 23.7%. Comparing with neat EAA, EAA mixed with DPS and DOP obtain a slightly higher crystallinity, while a lower extent was obtained in EAA/peanut oil. This is also mostly due to the difference in interaction between polymer and diluents molecules. The explanation to the influence of diluent addition on the crystallinity of EAA in mixture could be summarized as follows: (1) Molecular weight of diluent. The molecular weight of three diluents decreases in peanut oil > DOP > DPE. The one having a higher molecular weight hinders the EAA's chain segments arranging into lattice. (2) Inter-molecular interaction between diluent and the EAA. Peanut oil is a complex mixture of oleic oil, linoleic oil, and their glyceride. Polar groups on their molecules would have intense tangle with EAA's acrylic acid groups, which results in a hindrance to the crystallization of EAA. (3) Viscosity of homogeneous liquid mixture at melt state. High viscosity has negative effect on the movability of polymer chains. Although the EAA/peanut oil mixture has the lowest crystallization rate and crystallinity, the highest T_{m}^{p} indicates a more perfect spherulites structure in this mixture. Results discussed above in accordance with the highest Avrami exponent determined from Jeziorny's model analysis.

Based on our previous study on EAA/diluent microporous membrane study via TIPS process [46], it is suggested that non-isothermal crystallization starts right after the liquid–liquid phase separation process [8]. EAA/peanut oil mixture has the smallest pore size during the TIPS approach, while the EAA/DPE system has the largest scale at the same given EAA fraction.

Avrami index revealed that all crystallization of polymer in diluent environment derived from homogeneous nucleation. Nucleation process of EAA starts at the end of the liquid–liquid phase separation. The peanut oil has the largest molecular weight, as the diluent molecules are penetrated well into the matrix of EAA, it could insulate polymer chains with each other better, and this facilitates the homogeneous nucleation of EAA chain segments, which could explain the highest onset crystallization temperature of EAA in this mixture. Crystallization of EAA in EAA/peanut oil system

started at a comparative higher ambient temperature. This also results in a crystal structure with larger lamellar thickness, higher completion degree. The highest melting peak temperature of the corresponding subsequent melting endotherm is obtained. In conclusion, Avrami index value in this system from Jeziorny theory was highest.

The crystallization consists of the nucleation and the growth parts, and the overall crystallization rate depends on the competition relation between these two. As long as the temperature decreases to the onset crystallization temperature, relaxed chain segments starts to arrange onto the surface of existing nuclei. The nucleation of EAA in EAA/peanut oil system was faster than other two diluted systems. The most complex molecular structure, intense inter-molecular interaction derived from polar groups containing in polymer, and diluents would exist during EAA's crystallization.

It has been proposed that [47], as the non-isothermal crystallization behavior goes on, the solid–liquid phase separation proceeds at the same time. Diluent molecule could mostly exist in the liquid diluent rich phase outside the crystalline region. Besides, they could also be tangled within the polymer rich solid phase and fail to be repelled outside during the liquid–liquid phase separation period, and they would have apparent baffling effect on the chain segments' crystallizability. The non-isothermal crystallization rate parameters calculated from Jeziorny theory and Mo's approach show the EAA in EAA/peanut oil has the lowest value. As a result, the corresponding crystallinity integrated from subsequent melting thermal traces is the lowest. It can be suggested that the overall crystallization rate in EAA/diluent system is diffusion controlled.

Conclusions

In this article, non-isothermal crystallization kinetics of EAA during TIPS process in mixtures with peanut oil, DPE, and DOP diluents are investigated. The Jeziorny theory and the Mo's approach can obtain good linear fitting results of major primary crystallization. The Ozawa theory is not appropriate to describe this polymer/diluent system for its deficient consideration in secondary crystallization process. The effective activation energy of the EAA in mixture was estimated via Frieman's approach. Results revealed that it was easier for EAA to initialize crystallization at the beginning of cooling, while it became more difficult as the crystallization progress proceeded. Comparing with EAA in diluents mixtures, such growth tendencies in ΔE was more remarkable. The isolation effect from diluents insulated polymer chain sequences from tanglement with each other. In the homogeneous liquid mixture above melt temperature of EAA, molecules of diluent with smaller steric hindrance could more easily penetrate into the matrix of EAA, and

disperse randomly. They insulate the polymer's chains from each other. Results of Avrami index n show that EAA crystallizes in homogeneous nucleation mechanism and grows through three-dimensional growth geometry. The peanut oil diluted system has the highest Avrami index value, indicating a comparative higher insulation effect of EAA and a higher nucleation degree of freedom than other two diluents. The values of n in mixtures are all slightly higher than that in neat EAA case.

During the non-isothermal process, the molecular weight, polar groups, and complex molecular conformation play an important role in the crystallization kinetics of EAA. Peanut oil has the most complex molecular structure and the highest molecular weight. Carboxyl group on the oleic acid, linoleic acid, and their glycerides could have interaction with the acrylic acid units in EAA. Thus, the peanut diluted system has a stronger interaction between EAA and diluent molecules, and this would hinder the folding back movement of chain segments into the crystal lattices. Both non-isothermal crystallization rate parameters obtained from Jeziorny theory and Mo's method accord well with each other. Comparing with the crystallization of neat polymer, EAA crystallized slower in three diluted conditions. The EAA/peanut oil system has the slowest crystallization rate. The crystallization process in EAA/DPE system is faster than the other two systems, which is due to the simplest molecular structure and low molecular weight of DPE.

The subsequent melting behavior reveals that the peanut oil diluted EAA has the highest melt peak temperature, which is about 5 and 10 K above that of EAA/DOP and EAA/DPE systems, respectively. This indicates that the introducing of peanut oil facilitates the nucleation of EAA at higher temperature. More perfect crystals with bigger lamellar thickness are obtained. On the other hand, the lowest crystallinity is also obtained in EAA/peanut oil system, which should also be attributed to the influence of diluent molecule size.

References

1. Lim GBA, Kim SS, Ye Q, Wang YF, Lloyd DR. Microporous membrane formation via thermally induced phase separation. IV. Effect of isotactic polypropylene crystallization kinetics on membrane structure. *J Membr Sci*. 1991;64(1–2):31–40.
2. Yang MC, Perng JS. Microporous polypropylene tubular membranes via thermally induced phase separation using a novel solvent-camphephene. *J Membr Sci*. 2001;187(1):13–22.
3. Baltus RE. Characterization of the pore area distribution in porous membranes using transport measurements. *J Membr Sci*. 1997;123(2):165–84.
4. Hollman AM, Scherrer NT, Cammers-Goodwin A, Bhattacharyya D. Separation of dilute electrolytes in poly(amino acid) functionalized microporous membranes: model evaluation and experimental results. *J Membr Sci*. 2004;239(1):65–79.

5. Jeon MY, Kim CK. Phase behavior of polymer/diluent/diluent mixtures and their application to control microporous membrane structure. *J Membr Sci.* 2007;300(1–2):172–81.
6. Nunes SP, Peinemann KV. Ultrafiltration membranes from PVDF/PMMA blends. *J Membr Sci.* 1992;73(1):25–35.
7. Ochoa NA, Masuelli M, Marchese J. Effect of hydrophilicity on fouling of an emulsified oil wastewater with PVDF/PMMA membranes. *J Membr Sci.* 2003;226(1–2):203–11.
8. Gu MH, Zhang J, Wang XL, Tao HJ, Ge LT. Formation of poly(vinylidene fluoride) (PVDF) membrane via thermally induced phase separation. *Desalination.* 2006;192(11):160–7.
9. Wang S, Torkeson JM. Coarsening effects on the formation of microporous membrane produced via thermally induced phase separation of polystyrene-cyclohexanol solutions. *J Membr Sci.* 1995;98(3):209–22.
10. Shang MX, Matsuyama H, Teramoto M. Preparation and membrane performance of poly(ethylene-co-vinylalcohol) hollow fiber membrane via thermally induced phase separation. *Polymer.* 2003;44(24):7441–7.
11. Zhou J, Yin J, Lv R, Du Q, Zhong W. Preparation and properties of MPEG-grafted EAA membranes via thermally induced phase separation. *J Membr Sci.* 2005;267(1–2):90–8.
12. Zhou J, Lin Y, Du Q, Zhong W, Wang H. Effect of MPEG on MPEG-grafted EAA membrane formation via thermally induced phase separation. *J Membr Sci.* 2006;283(1–2):310–9.
13. Kolesov IS, Androsch R, Radusch HJ. Non-isothermal crystallization of polyethylenes as function of cooling rate and concentration of short chain branches. *J Therm Anal Calorim.* 2004;78(3):885–95.
14. Parasnis NC, Ramani K. Non-isothermal crystallization of UHMWPE. *J Therm Anal Calorim.* 1999;55(3):709–19.
15. Vyazovkin S, Sbirrazzuoli N. Estimating the activation energy for non-isothermal crystallization of polymer melts. *J Therm Anal Calorim.* 2003;72(2):681–6.
16. Alvarez VA, Stefani PM, Vazquez A. Non-isothermal crystallization of polyvinylalcohol-co-ethylene. *J Therm Anal Calorim.* 2005;79(1):187–93.
17. Zhang J, Chen SJ, Su J, Shi XM, Jin J, Wang XP, et al. Non-isothermal crystallization kinetics and melting behavior of EAA with different acrylic acid content. *J Therm Anal Calorim.* 2009;97(3):959–67.
18. Gu MH, Zhang J, Wang XL. Crystallization behavior of PVDF in PVDF-DMP system via thermally induced phase separation. *J Appl Polym Sci.* 2006;102(4):3714–9.
19. Tao HJ, Zhang J, Wang XL. Phase separation, polymer crystallization in TPX-DOS -DMP system via thermally induced phase separation. *J Polym Sci B.* 2007;45(2):153–61.
20. Brandrup J, Immergut EH. Polymer handbook. New York: Wiley; 1999.
21. Lloyd DR, Kim SS, Kinzer KE. Microporous membrane formation via thermally induced phase separation. II. Liquid–liquid phase separation. *J Membr Sci.* 1991;64(1–2):1–11.
22. Matsuyama H, Maki T, Teramoto M. Effect of polypropylene molecular weight on porous membrane formation by thermally induced phase separation. *J Membr Sci.* 2002;204(1–2):323–8.
23. McGuire KS, Laxminarayan A, Lloyd DR. Simple method of extrapolating the coexistence curve and predicting the melting point depression curve from cloud point data for polymer-diluent systems. *Polymer.* 1994;35(20):4404–7.
24. Zhang J, Fu J, Wang XL. Effect of diluents on hydrophilic ethylene-acrylic acid co-polymer membrane structure via thermally induced phase separation. *Desalination.* 2006;192(1–3):151–9.
25. Cebe P, Hong SD. Crystallization behavior of poly (ether-ether-ketone). *Polymer.* 1986;27(8):1183–92.
26. Avrami M. Kinetics of phase change (I): general theory. *J Chem Phys.* 1939;7(12):1103–12.
27. Avrami M. Kinetics of phase change (II): transformation-time relations for random distribution of nuclei. *J Chem Phys.* 1940;8(2):212–24.
28. Avrami M. Granulation, phase change and microstructure. *J Chem Phys.* 1941;9(2):177–84.
29. Jeziorny A. Parameters characterizing the kinetics of the non-isothermal crystallization of poly(ethylene terephthalate) determined by DSC. *Polymer.* 1978;19(10):1142–4.
30. Huang JW, Chang CC, Kang CC, Yeh MY. Crystallization kinetics and nucleation parameters of Nylon 6 and poly(ethylene-co-glycidyl methacrylate) blend. *Thermochim Acta.* 2008;468(1–2):66–74.
31. Rychly J, Janigova I. Avrami equation and nonisothermal crystallization of polyethylene investigated by DSC. *Thermochim Acta.* 1993;215:211–8.
32. Shi XM, Jin J, Chen SJ, Zhang J. Multiple melting and partial miscibility of ethylene-vinyl acetate copolymer/low density polyethylene blends. *J Appl Polym Sci.* 2009;113(5):2863–71.
33. Liu MY, Zhao QX, Wang YD, Zhang CG, Mo ZS, Cao SK. Melting behaviors, isothermal and non-isothermal crystallization kinetics of nylon 1212. *Polymer.* 2003;44(8):2537–45.
34. Choe CR, Lee KH. Nonisothermal crystallization kinetics of poly(etheretherketone) (PEEK). *Polym Eng Sci.* 1989;29(12):801–5.
35. Ozawa T. Kinetics of non-isothermal crystallization. *Polymer.* 1971;12(3):150–8.
36. Xu JT, Wang Q, Fan ZQ. Non-isothermal crystallization kinetics of exfoliated and intercalated polyethylenemontmorillonite nanocomposites prepared by in situ polymerization. *Eur Polym J.* 2005;41(12):3011–7.
37. Liu TX, Mo ZS, Wang S, Zhang H. Nonisothermal melt and cold crystallization kinetics of poly(aryl ether ether ketone ketone). *Polym Eng Sci.* 1997;37(3):568–71.
38. Zhang QX, Zhang ZH, Zhang HF, Mo ZS. Isothermal and non-isothermal crystallization kinetics of nylon-46. *J Polym Sci B.* 2002;40(16):1784–93.
39. Kissinger HE. Variation of peak temperature with heating rate in differential thermal analysis. *J Res Natl Bur Stand.* 1956;57(4):217–21.
40. Vyazovkin S. Modification of the integral isoconversional method to account for variation in the activation energy. *J Comput Chem.* 2001;22(2):178–83.
41. Vyazovkin S, Sbirrazzuoli N. Isoconversional analysis of calorimetric data on nonisothermal crystallization of a polymer melt. *J Phys Chem B.* 2003;107(3):882–8.
42. Vyazovkin S, Dranca I. Isoconversional analysis of combined melt and glass crystallization data. *Macromol Chem Phys.* 2006;207(1):20–5.
43. Qudah AMA, Al-Raheil IA. Morphology and melting behaviour of poly(ethylene terephthalate) crystallized from the glassy state. *Polym Int.* 1995;38(4):367–73.
44. McGuire KS, Laxminarayan A, Lloyd DR. Kinetics of droplet growth in liquid–liquid phase separation of polymer-diluent systems: experimental results. *Polymer.* 1995;36(26):4951–60.
45. Shen M, Mehra U, Niinomi M, Koberstein JT, Cooper SL. Morphological, rheo-optical, and dynamic mechanical studies of a semicrystalline block copolymer. *J Appl Phys.* 1974;45(10):4182–9.
46. Zhang J, Luo F, Wang XL, Chen JF, Xu ZZ. The effect of kinetic factors on the structure of the hydrophilic ethylene-acrylic acid copolymer microporous membranes prepared via thermally induced phase separation. *Acta Polym Sin.* 2003;42(2):241–6.
47. Laxminarayan A, McGuire K, Kim S, Lloyd D. Effect of initial composition, phase separation temperature and polymer crystallization on the formation of microcellular structures via thermally induced phase separation. *Polymer.* 1994;35(14):3060–8.